Multiscale mathematical biology of cell-extracellular matrix interactions during morphogenesis

Rens, E.G.

5

Mathematical Modeling of the Nodal Signaling Range Regulated by FurinA induced Nodal Maturation

This chapter presents the mathematical modeling aspects of

Tessadori F, Noël ES, **Rens EG**, Magliozzi R, Evers-van Gogh IJA, Guardavaccaro D, Merks RMH, and Bakkers J (2015) *Nodal Signaling Range Is Regulated by Proprotein Convertase-Mediated Maturation*. Developmental Cell 32(5): 631-639.

Abstract

Morphogens that diffuse through tissues drive tissue patterning. In many animal species, left-right patterning is governed by a reaction- diffusion system relying on the different diffusivity of an activator, Nodal, and an inhibitor, Lefty. In a genetic screen, a zebrafish loss of function mutant for the proprotein convertase FurinA was identified. The Spaw protein in zebrafish is a Nodal-related proprotein and is able to induce its own expression trough extracellular signaling. Embryological and biochemical experiments demonstrate that FurinA cleaves the Nodal-related Spaw proprotein into a mature form. This mature form can then be secreted and diffuse, allowing for long range Nodal signaling. We developed a model that describes inter and extracellular Nodal dynamics and included cleavage by FurinA. This mathematical shows that FurinA is required for Spaw gradient formation. The model suggests that the speed of gradient formation and the range of Spaw signaling is regulated by FurinA, which is validated by *in vivo* experiments. Finally, the model suggests that the effect of FurinA saturates with increasing levels of FurinA. This study shows that tissue patterning, such as left-right patterning, can be regulated by proprotein convertases.

5.1 Introduction

In the previous chapters, we focused on how mechanical forces can drive tissue patterning. Cells sense and respond to mechanical forces that are present in the extracellular matrix. However, cells also respond to chemical signals from the extracellular matrix. For decades, tissue patterning has been thought to be mainly regulated by morphogens, chemical signals or growth factors diffusing through the extracellular space, that affect the gene transcription of cells. In this chapter, we focus on how chemical signaling is involved in the left-right patterning of tissues. During embryogenesis, an asymmetry between the left and right part of the body is established. This left-right (LR) assymetry is crucial for the formation, positioning and function of organs [261]. During somitogenesis, the vertebrate LR axis is patterned by the interplay of Nodal and its repressor Lefty [262, 263]. Nodal and Lefty form a activator/inhibitor pair and have different diffusivities, activation ranges. As such, the pair behaves as a reaction-diffusion model for tissue patterning. Lefty inhibits the expression of Nodal and Nodal induces its own expression. An initial assymetry between left and right, caused by the accumulation of Nodal in the left lateral plate mesoderm (LMP) (due to cilia-induced flow in the node), is amplified by the Nodal/Lefty interactions [261]. Since Lefty acts on a long range, the expression of Nodal is repressed in the right side of the body.

Nodal is an extracellular protein that induces its own gene expression, by signaling through cell membrane receptors. Nodal protein can only be secreted by cells once it matures, which is regulated by proprotein convertases such as Furin. In this chapter, we focus on the model system zebrafish to study the signaling range of Nodal. In zebrafish, the Nodal gene southpaw (Spaw) is required for LR patterning. At early somatogenesis, Spaw expression is initiated around the posteriorly localized Kupffer's vesicle, which

is the functional homolog to the mouse's node [264]. Experimental studies on the ace of hearts (aoh), a zebrafish mutant for the proprotein convertase FurinA, shows that Spaw acquires its biological activity and signaling range via FurinA-mediated maturation. A combination of *in vivo* and *in silico* experiments shows that the level of FurinA expression in the zebrafish embryo controls the signaling range of Spaw.

5.1.1 Zebrafish aoh mutant

Tessadori *et al.* [98] identified a zebrafish mutant that displayed a defect in left-right patterning; it had a midline-positioned cardiac tube, which is normally located at the left side. This mutant is called the aoh mutant. For more details, we refer to the original paper [98]. In this chapter, we only describe the most relevant observations for the mathematical modeling. The left-right defect was due to a reduced expression of the gene Spaw in the LPM (Figure 5.1). But what characteristic of this mutant affected the signaling range of Spaw?

It was determined that aoh mutants carry a point mutation resulting in a premature truncation of the FurinA subtilisin-like proprotein convertase (SPC). Furin is part of a larger family of SPCs, which are crucial for conferring biological functionality to a wide variety of substrates including growth factors belonging to the Tgf-β superfamily [265, 266]. To confirm that the lack of FurinA is responsible for reduced Nodal signaling, additional experiments were performed. This showed that FurinA can cleave Nodal and that the *in vitro* addition of Furin protein resulted in the efficient cleavage of Spaw. By *in vivo* mutation of cleavage sites of Spaw, it was shown that if Furin could not cleave Spaw, the function of Spaw was abrogated.

5.1.2 The role of FurinA

Studies showed that Spaw induces the activity of Spaw [267] and that Spaw acts on a long range [98]. Furthermore, it was shown that the cell-autonomous cleavage of Spaw by FurinA is required for this long range signaling [98]. Localization of Spaw maturation by FurinA correlates positively with extracellular Spaw localization and thus mediates the formation of an extracellular Spaw gradient [98]. To understand how FurinA processing of Spaw controls the establishment of the Nodal signaling domain in the LPM during LR patterning, we developed a mathematical model.

5.2 Model description

The mathematical model considers the intercellular and extracellular Spaw protein dynamics and their interactions in a 1D domain. The domain represents an embryonic tissue, where $x = 0$ corresponds to the source of Nodal and $x = L$ represents the boundary of the relevant tissue.

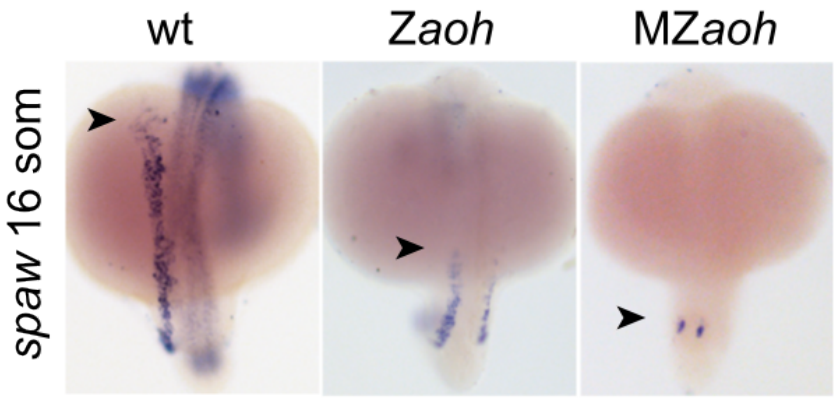

Figure 5.1: Expression of Spaw (arrowhead indicates anterior-ward expansion) in WT, Zaoh, and MZaoh embryos.

The model is given by the following reaction-diffusion system

$$\frac{\partial S_i}{\partial t} = \underbrace{cm_e \frac{\frac{S_e}{h_e}}{1+\frac{S_e}{h_e}}}_{\text{production}} - \underbrace{\epsilon_i S_i}_{\text{degradation}} - \underbrace{kFS_i}_{\text{maturation}}, \tag{5.1}$$

$$\frac{\partial S_i^m}{\partial t} = \underbrace{kFS_i}_{\text{maturation}} - \underbrace{\epsilon_i^m S_i^m}_{\text{degradation}} - \underbrace{sS_i^m}_{\text{secretion}}, \tag{5.2}$$

$$\frac{\partial S_e}{\partial t} = \underbrace{D\nabla^2 S_e}_{\text{diffusion}} - \underbrace{\epsilon_e S_e}_{\text{degradation}} + \underbrace{sS_i^m}_{\text{secretion}}, \tag{5.3}$$

with boundary conditions,

$$\frac{\partial S_e}{\partial x}(x=L,t) = 0, \tag{5.4}$$

$$D\frac{\partial S_e}{\partial x}(x=0,t) = -P, \tag{5.5}$$

and initial conditions,

$$S_i(x,t=0) = 0, \tag{5.6}$$

$$S_i^m(x,t=0) = 0, \tag{5.7}$$

$$S_e(x,t=0) = 0. \tag{5.8}$$

Here, $S_i(x,t)$, $S_i^m(x,t)$ and $S_e(x,t)$ denote the concentration (in molecules/liter) of synthesized intercellular Spaw, mature intercellular Spaw and extracellular Spaw, respectively. The model takes into account that the extracellular Spaw diffuses with

diffusion coefficient D (m^2s^{-1}) and degrades with an extracellular clearance rate of ϵ_e (s^{-1}). Further, the intracellular Spaw degrades with an intercellular clearance rate of ϵ_i (s^{-1}) and ϵ_i^m (s^{-1}) for its mature form. The mature form of Spaw is secreted with a rate s (s^{-1}). Spaw only spreads between cells through the extracellular space, so there is no diffusion of $S_i(x,t)$ or $S_i^m(x,t)$. We assume that FurinA promotes the maturation of Spaw. This is represented by the term kFS_i, present in both of the intercellular Spaw equations. Here, F is the concentration of FurinA (molecules/liter) and k is a constant. We thus assume that the rate of maturation, which is kF (s^{-1}), is linearly dependent on the level of FurinA.

The model describes the production of intercellular Spaw, at a maximum of cm_e (s^{-1} molecules/liter), in response to the cells' binding of extracellular Spaw. We assume that this activation of intercellular protein production becomes saturated when the level of $S_e(x,t)$ increases, as then the number of receptors sensing the extracellular Spaw depletes. This is indicated by the Michaelis-Menten kinetics function, where m_e and h_e are constants. More specifically, m_e is the extracellular Spaw concentration at which all Spaw receptors of the cells are occupied and h_e is the extracellular Spaw concentration at which the synthesis activation rate is at half-maximum.

The boundary condition at $x = L$ reflects the fact that extracellular Spaw can not leave the tissue. At $x = 0$, we assume a constant influx of P (molecules s^{-1} m^{-2}) of extracellular Spaw. As initial conditions, we assumed $S_e(x,t) = S_i(x,t) = S_i^m(x,t) = 0$; that is, at no extracellular or intracellular Spaw is present anywhere in the domain.

5.3 Results

The results and comparison with *in vivo* data of the mathematical model are shown in Figure 5.2; the mathematical equations are shown in Figure 5.2). In brief, in this one-dimension reaction-diffusion model (Figures 5.2A and 5.2B), the maturation of Spaw is controlled by FurinA processing. Once processed, Spaw is secreted and forms an extracellular gradient. Extracellular mature Spaw diffuses to surrounding cells, where it binds to its receptor and stimulates the production of intracellular Spaw. Both intracellular and extracellular Spaw are assumed to be degraded according to first order kinetics, *i.e.*, due to proteolysis independent of Spaw or FurinA.

5.3.1 FurinA expression levels controls speed and range of Spaw gradient formation

The model produces a front of extracellular, mature Spaw protruding into the LPM, with a propagation speed that is enhanced by the level of FurinA. In Movie S1, snapshots of which are shown in Figure 5.2D, the faster propagation of extracellular Spaw resulting from an increase in FurinA levels can be appreciated. The mathematical model predicts that the distance reached by a specific amount of extracellular Spaw within a given time is a function of FurinA levels (Figure 5.2E). Due to its self-inducing activity, we used the Spaw expression domain as a readout for extracellular Spaw ac-

tivity *in vivo*. With increasing FurinA levels, the model predicts an increasing anterior extension of the Spaw expression domain at a given developmental stage. To test this prediction *in vivo*, we determined the signaling range of Spaw in the LPM by measuring the length of the Spaw expression domain in embryos with different levels of FurinA (Figure 5.2F). First, we compared the Spaw expression domain in embryos with no FurinA (MZaoh mutant), low levels of FurinA (Zaoh), and normal FurinA expression (wild-type [WT] embryos). In agreement with the prediction of the mathematical model, we observed that the Spaw expression domain in the LPM was absent in the MZaoh mutant embryos, while the extension of the Spaw expression domain was limited in Zaoh mutant embryos, which is consistent with its expression in the posterior, but not in the anterior LPM.

Next, we examined whether increasing FurinA levels in WT embryos would be sufficient to expand the signaling range of Spaw even further in the anterior direction, as the mathematical model predicts. Since endogenous FurinA is broadly expressed at early developmental stages and during somitogenesis [268], we overexpressed FurinA in all cells by mRNA injection into WT embryos and determined the anterior-posterior length of the Spaw expression domain. We observed that increasing FurinA was sufficient to induce an expansion of the signaling range of Spaw (Figure 5.2F). Interestingly, increased FurinA expression levels resulted not only in faster expansion of Spaw expression toward the anterior LPM, but also in an increased incidence of bilateral Spaw expression and the appearance of right-sided Spaw expression in the LPM. This could be the consequence of the saturation of the midline barrier and of the activity of a self-enhancement lateral-inhibition system, as described for mouse Nodal and Lefty [269] (Figure 5.2F; see Nakamura *et al.*, 2006). Altogether, we conclude that the level of FurinA determines the signaling range of Spaw in the LPM, which is critical for the establishment of correct LR patterning of the embryo.

5.3.2 Signaling range saturates by increasing level of FurinA

Increasing FurinaA levels, F in the model, leads to an increase of extracellular Spaw, as its promotes maturation of Spaw that can subsequently be secreted. The amount of Spaw maturation depends on the production rate of intercellular Spaw, so the effect of increasing F is likely limited. In order to better understand the effect of F, we linearized the original model to

$$\frac{\partial S_i}{\partial t} = cS_e - \epsilon_i S_i - kFS_i, \tag{5.9}$$

$$\frac{\partial S_i^m}{\partial t} = kFS_i - \epsilon_i^m S_i^m - sS_i^m, \tag{5.10}$$

$$\frac{\partial S_e}{\partial t} = D\nabla^2 S_e - \epsilon_e S_i + sS_i^m, \tag{5.11}$$

with the same boundary conditions and initial conditions as described in the model formulation given in the methods section.

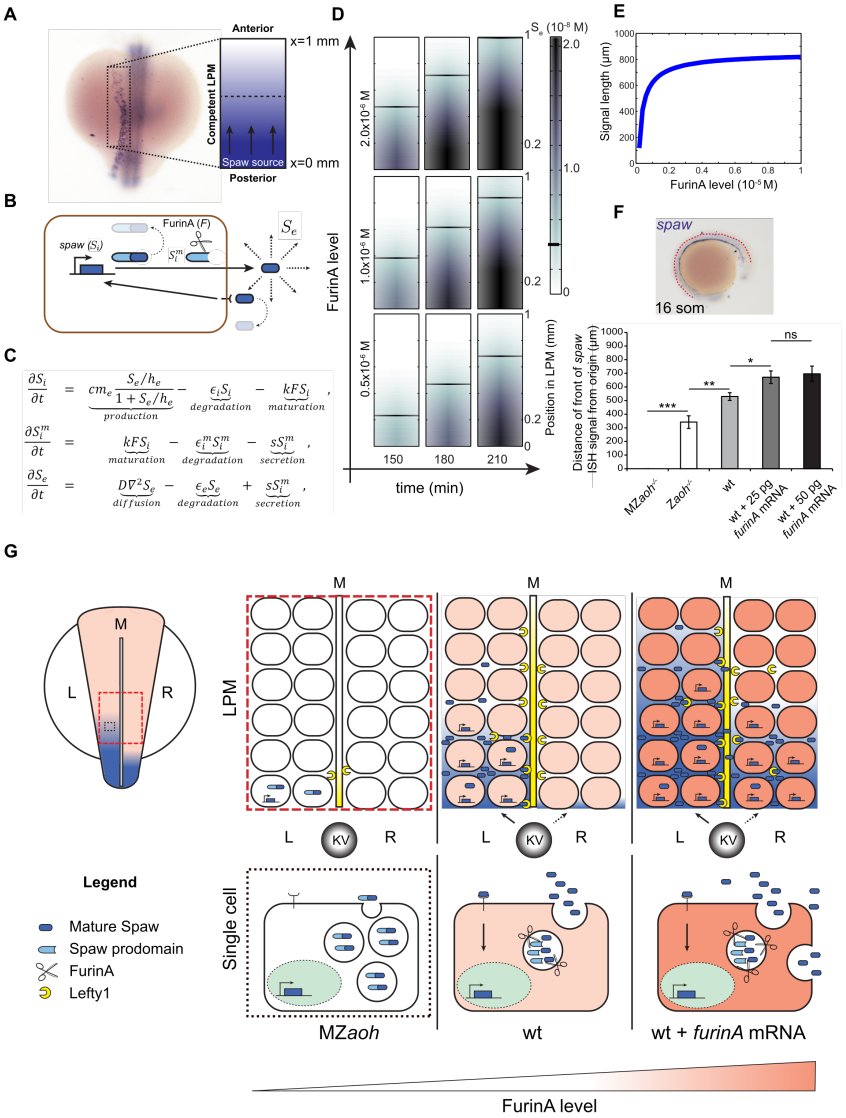

Figure 5.2: Caption is on next page

Caption of figure on previous page: FurinA Levels Control the Expansion of the Spaw Expression Domain in the LPM. (A and B) For the purpose of mathematical modeling, we have considered the left LPM of the developing zebrafish embryo as a linear domain (displayed as a rectangle here) with a source of Spaw at the posterior end (x = 0); (B) behavior of Spaw in the competent LPM described in (A). Synthetized intracellular Spaw (S_i), mature intracellular Spaw (S_i^m), and extracellular Spaw (S_e). (C) Partial-differential equation model of the system described in (B). (D) Snapshots of Movie S1 showing a simulation of the model defined in (C). The speed of progression of Se, and consequently of the domain of Spaw expression in the LPM, increases with the level of FurinA. (E) The model predicted that increasing FurinA levels, resulting in enhanced maturation of Spaw, results in increased length of the Spaw expression domain at a given time (180 min here). (F) Quantification of the length of the Spaw expression domain (anterior-posterior) in embryos with no (MZaoh; n = 12), low (Zaoh mutants; n = 7), normal (WT; n = 15), or high (WT injected respectively with 25 pg; n = 25 and 50 pg; n = 17 FurinA mRNA) FurinA levels. Histograms display average value Âś SEM; *p < 0.05, **p < 0.01, and ***p < 0.005 in Student's t test. (G) Cartoon illustrating the effect of FurinA on the signaling range of Spaw in the LPM. In a WT situation, Spaw is cleaved prior to secretion by cells at the posterior end of the LPM (10 somite stage, 13 hpf). Spaw induces its own expression in a paracrine fashion, and the Spaw expression domain expands toward the anterior end of the developing LPM, reaching the heart field at the 23-somite stage (20 hpf). Spaw also induces expression of *Lft1* at the midline, which prevents it from reaching the right LPM. Spaw expression is consequently limited to the left LPM and establishes LR patterning. In the MZaoh mutants, the absence of FurinA processing of Spaw results in failure to induce Spaw expression in the LPM and of *Lft1* in the midline. As a consequence, LR patterning is affected. Overexpression of FurinA results in increased presence of mature Spaw in the extracellular space. The activation of Spaw in the LPM progresses faster toward the anterior left LPM. LR patterning is affected, likely as a result of an excess of Spaw protein overcoming the Lft1 midline barrier, Kupffer's Vesicle (KV) and midline (M).

Let us first consider the steady state solution, which is obtained by solving

$$\frac{\partial S_i}{\partial t} = 0, \tag{5.12}$$

$$\frac{\partial S_i^m}{\partial t} = 0, \tag{5.13}$$

$$\frac{\partial S_e}{\partial t} = 0, \tag{5.14}$$

or,

$$cS_e - \epsilon_i S_i - kFS_i = 0, \tag{5.15}$$

$$kFS_i - \epsilon_i^m S_i^m - sS_i^m = 0, \tag{5.16}$$

$$D\nabla^2 S_e - \epsilon_e S_e + sS_i^m = 0. \tag{5.17}$$

This can be rewritten to

$$D\nabla^2 S_e + \alpha S_e = 0 \tag{5.18}$$

with simply

$$S_i(x) = \frac{c}{\epsilon_i + kF} S_e(x), \tag{5.19}$$

$$S_i^m(x) = \frac{kF}{\epsilon_i^m + s} S_i(x). \tag{5.20}$$

Here, α is given by $\alpha = \frac{sc}{\epsilon_i^m + s} \frac{kF}{\epsilon_i + kF} - \epsilon_e$.
The case $\alpha > 0$ represents a system where the production of Spaw exceeds Spaw's extracellular degradation rate. This implies that no steady state exists. Thus, for high values of c, the level of extracellular Spaw will increase indefinitely in the linear model. For this reason, we take this case out of consideration in this analysis. We also omit the case $\alpha = 0$, because it can generally only be obtained when $\epsilon_e = 0 \wedge (c = 0 \vee s = 0 \vee F = 0)$, which are all irrelevant cases, because then only diffusion of extracellular Spaw is present. For $\alpha < 0$, we obtain the steady state solution

$$S_e(x) = C_1 \exp(-\sqrt{|\alpha|/D}x) + C_2 \exp(\sqrt{|\alpha|/D}x), \tag{5.21}$$

where C_1 andC_2 are constants of integration. These constants are given by the prescribed boundary conditions. We find the following expressions for the constants C_1 and C_2:

$$C_2 = \frac{\frac{-P}{D}}{\sqrt{|\alpha|/D}} + C_1, \tag{5.22}$$

$$C_1 = -\left(\frac{\frac{-P}{D}}{\sqrt{|\alpha|/D}}\right) \cdot \frac{\exp(\sqrt{|\alpha|/D})}{\exp(\sqrt{-|\alpha|/D}) - \exp(\sqrt{|\alpha|/D})}. \tag{5.23}$$

Note that in order to have $\alpha < 0$ for all values of F, we need that $c < \epsilon_e$. Figure 5.3 shows the steady states for $c = 90 \cdot 10^{-6}$, $\epsilon_e = 100 \cdot 10^{-6}$ and a range of values for F. The extracellular Spaw concentration in the domain correlates positively with the level of FurinA. To get an idea of how exactly the total concentration reached in the domain, is influenced by F, we consider the total amount of extracellular Spaw in the system at time t [270], which is given by

$$N_e(t) = \int_0^{x=L} S_e(x,t)dx. \tag{5.24}$$

Analogously, let the total amount of intercellular Spaw be denoted by

$$N_i(t) = \int_0^{x=L} S_i(x,t)dx, \tag{5.25}$$

$$N_i^m(t) = \int_0^{x=L} S_i^m(x,t)dx. \tag{5.26}$$

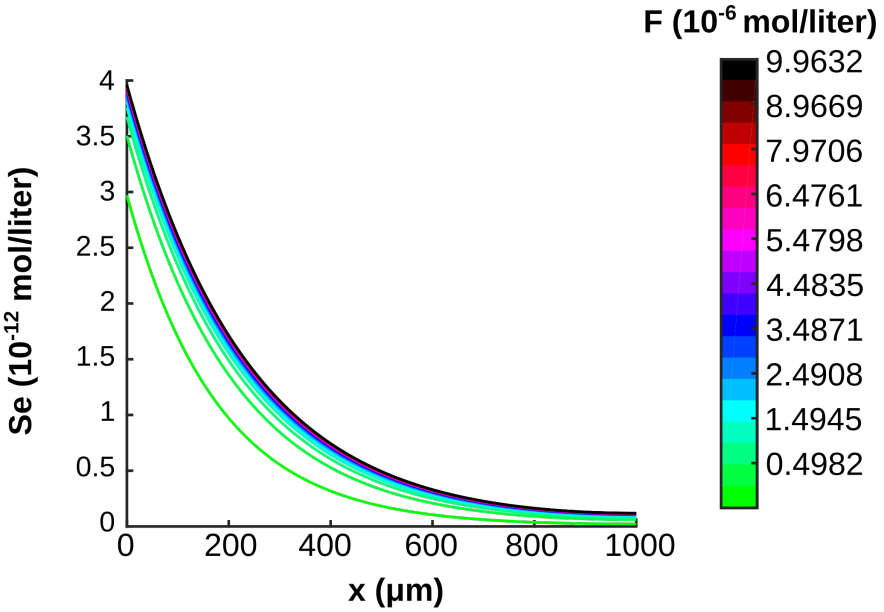

Figure 5.3: Steady state extracellular Spaw (S_e) concentration gradients over domain x = [0, 1000 μm] as a function of FurinA (F) concentration (color bar)

Now,

$$\frac{dN_e}{dt} = \int_0^{x=L} \frac{\partial S_e}{\partial t} dx, \tag{5.27}$$

$$= D \int_0^{x=L} \nabla^2 S_e dx - \epsilon_e \int_0^{x=L} S_e dx + s \int_0^{x=L} S_i^m dx, \tag{5.28}$$

$$= D[\nabla S_e]_0^{x=L} - \epsilon_e N_e(t) + s N_i^m(t), \tag{5.29}$$

$$= P - \epsilon_e N_e(t) + s N_i^m(t), \tag{5.30}$$

and similarly,

$$\frac{dN_i}{dt} = cN_e(t) - (\epsilon_i + kF)N_i(t) \tag{5.31}$$

$$\frac{dN_i^m}{dt} = kFN_i(t) - (\epsilon_i^m + s)N_i^m(t) \tag{5.32}$$

In steady state we have that

$$\frac{dN_e}{dt} = 0, \tag{5.33}$$
$$\frac{dN_i}{dt} = 0, \tag{5.34}$$
$$\frac{dN_i^m}{dt} = 0, \tag{5.35}$$

or,

$$P - \epsilon_e N_e(t) + sN_i^m(t) = 0, \tag{5.36}$$
$$cN_e(t) + (\epsilon_i + kF)N_i(t) = 0, \tag{5.37}$$
$$kFN_i(t) + (\epsilon_i^m + s)N_i^m(t) = 0, \tag{5.38}$$

which gives the following expression for $N_e(t)$

$$N_e(t) = \frac{-P}{\frac{sc}{\epsilon_i^m+s}\frac{kF}{\epsilon_i+kF} - \epsilon_e} = \frac{-P}{\alpha}. \tag{5.39}$$

This shows that a higher F implies a higher total amount of extracellular Spaw in steady state condition (as we assumed that $\alpha < 0$). However, this influence of F saturates with increasing levels of FurinA. This can be explained by the following observation: $lim_{F\to\infty}\alpha = lim_{F\to\infty}\frac{sc}{\epsilon_i^m+s}\frac{kF}{\epsilon_i+kF} - \epsilon_e = \frac{sc}{\epsilon_i^m+s} - \epsilon_e$, indicating that increasing F will ultimately not change the system behavior. Increasing FurinA only helps to increase the extracellular Spaw to a certain point, as it is limited by the intercellular production rate. Notably, the magnitude of the effect of Fon the system depends on the value of c. The higher the c, the larger the effect of F. In other words, with a lower value for c , the convergence due to F is faster. This is because how much Spaw is produced within the cell, limits the amount of mature Spaw. In conclusion, by regulating the maturation of intercellular Nodal, FurinA regulates the signaling range of Nodal. Increasing FurinA increases the signaling range, upto a maximum range determined by the maximum rate of intercellular production of Nodal.

5.4 Discussion

Based on experimental studies we developed a model that shows that cleavage of the Nodal-related Spaw proprotein into a mature form by FurinA is required for the formation of an extracellular Spaw gradient. In this model, extracellular Spaw induces intercellular Spaw production, which is cleaved by FurinA into a mature form that can be secreted and diffuse through the extracellular matrix. This diffusion allows for long range cell-cell signaling. In the absence of FurinA, this signaling can not take place. Increasing FurinA speeds up gradient formation and creates a longer signaling range, which has been validated with *in vivo* experiments. The model suggests that this positive effect of FurinA saturates, as the production of intercellular Spaw is bounded

by the number of Spaw receptors that enable extracellular Spaw signaling. This study shows that proprotein convertase FurinA is essential for Spaw signaling, which in turn is essential for correct establishment of LR patterning and organ laterality.

We demonstrated how FurinA acts as a regulator of LR patterning by controlling the signaling range of Spaw. Signaling ranges are typically controlled by diffusion and reaction. This work suggests a new mechanism that also controls extracellular gradient formation: the maturation of intercellular proteins.

5.5 Supplementary methods

5.5.1 Numerical analysis

For the numerical simulations, we used a backward Euler scheme in time and a second-order central difference scheme in space, with spatial discretization sizes of $\Delta x = \frac{L}{1000}$ and time steps of $\Delta t = 15s$. The simulation ends when time t_{end} is reached. In order to evaluate the time it takes for the system to reach a given state, we need to define a position in the domain, denoted by x_{signal}, at which we test if the concentration of extracellular Spaw exceeds a threshold level of extracellular Spaw, $S_e^{threshold}$. So, more specifically, we determine $t_{\text{signal}}(x) = min\{t : S_e(x_{\text{signal}}, t) > S_e^{\text{threshold}}\}$. We also identify how far the signal has extended at each point in time, as $x_{\text{signal}}(t) = min\{x : S_e(x, t) < S_e^{\text{threshold}}\}$. These measures help illustrate how FurinA speeds up the extracellular Spaw propagation.

5.5.2 Parameter value estimation

Values for parameters were either adopted from literature, or estimated based on our data. The parameter values are given in Table 5.1. The length of the tissue and the simulation duration is based on our data. The parameters D and ϵ_e are chosen according to values for the protein Squint as described in [271], because Spaw protein dynamics are comparable to Squint. The constant k, a measure of how efficiently FurinA converts Spaw into its mature form, is assumed to be 10^{-4} s^{-1} liter/mol, which is comparable to typical values for various enzymes [272]. The concentration of FurinA in the system was estimated using our data as follows. We consider an injection of 25 pg of FurinA mRNA in 200 nl and assume a translational efficiency of 10^3 [273], which gives us a FurinA protein concentration of 10^{-6} mol/liter. The influx P of extracellular Spaw was estimated based on HER2 secretion rates in [274]. Here, 1500 pg of HER2 was secreted into 1 ml of medium by $3 \cdot 10^5$ mammalian cells in 24 hours. We assume that the secreted protein is transported over at membrane of one spherical cell with radius $5\mu m$. With these values, we obtain an influx of in the order of 10^{-8} mol m^{-2} s^{-1} The values for h_e and m_e were estimated based on the lower range of the concentrations of signaling molecules, of around 10 nM (BioNumbers.org). The $S_e^{\text{threshold}}$ was chosen such that this threshold could not be reached in the absence of FurinA, in correspondence to the experiments. The parameters s and ϵ_i^m were given the same value as ϵ_e. The parameters

ϵ_i and c were chosen such that the time it takes for the modeled system to reach a certain state in the presence of FurinA is similar to our data. To be more specific, these parameters were chosen such that after 180 min, the signal is roughly between 0 and 700 μm and the time it takes for the signal to reach 1000 μm is roughly between 180 and 360 min. Within the limits identified using the theoretical analysis of the linearized model, however, the overall behavior of the non-linear system described here does not depend on the specific choice of parameter values. Further, we would like to point out that we assume a round number of molecules for a number of parameters. We divide these by Avogadro's number, yielding the non-intuitive molarity values.

5.6 Supplementary tables

parameter	description	value	unit
Δx	Spatial discretization stepsize	1	µm
Δt	Time discretitazion stepsize	15	s
L	Length of tissue	1000 (data)	µm
t_{end}	Simulation end	360 (data)	min
D	Diffusion coefficient	3.2 [271]	$\mu m^2\ s^{-1}$
ϵ_e	Extracellular clearance rate	$1 \cdot 10^{-4}$ [271]	s^{-1}
ϵ_i	Intercellular clearance rate	$75 \cdot 10^{-4}$	s^{-1}
ϵ_i^m	Intercellular clearance rate for mature form	$1 \cdot 10^{-4}$	s^{-1}
c	Synthesis activation rate	$200 \cdot 10^{-4}$	s^{-1}
s	Secretion rate	$1 \cdot 10^{-4}$	s^{-1}
k	Constant that relates level of FurinA to rate of Spaw maturation	10^4 [272]	s^{-1}liter/mol
F	FurinA concentration	ranges from 0 to $5{\cdot}10^{-6}$ (data, [273])	mol/liter
h_e	Extracellular Spaw concentration at which the synthesis activation rate is at half-maximum	$4.15 \cdot 10^{-10}$	mol/liter
m_e	Concentration of extracellular Spaw at which all Spaw receptors of the cells are occupied	$8.3 \cdot 10^{-10}$	mol/liter
P	Extracellular Spaw flux	$1.66 \cdot 10^{-8}$	mol $m^{-2}s^{-1}$ [274]
$S_e^{\text{threshold}}$	Signalling threshold	$4.15 \cdot 10^{-10}$	mol/liter

Table 5.1: Parameter settings.

5.7 Supplementary videos

Video S1 shows numerical simulations of the progression of extracellular Spaw (S_e) and, subsequently, of the domain of spaw expression in the LPM, in the presence of increasing levels of FurinA. It can be found at `http://dx.doi.org/10.1016/j.devcel.2014.12.014`